



DFT Studies on Ethane Activation by Gas-Phase PtX⁺ (X = F, Cl and Br)

XI-LONG MA, JUN MA, KAI-LI ZHU and ZHI-YUAN GENG*

Gansu Key Laboratory of Polymer Materials, College of Chemistry and Chemical Engineering, Key Laboratory of Eco-environment-Related Polymer Materials, Ministry of Education, Northwest Normal University, Lanzhou 730070, Gansu Province, P.R. China

*Corresponding author: Fax: +86 931 7971989; E-mail: zhiyuangeng@126.com

Received: 21 January 2015;

Accepted: 2 March 2015;

Published online: 26 May 2015;

AJC-17270

The mechanism of C-H bond activation of C₂H₆ catalyzed by platinum halide cations [PtX⁺ (X = F, Cl and Br)] has been carried out at the DFT (B3LYP) level based on the RECP + 6-311+G(d,p). Both high-spin and low-spin potential energy surfaces are characterized. For PtCl⁺/C₂H₆ and PtBr⁺/C₂H₆ system, the crossing point between the different potential-energy surfaces is required. For PtF⁺/C₂H₆ couple, the whole reaction proceeds on the ground-states potential energy surfaces with a spin-allowed manner. Our calculations indicate that the reactions take place more easily along the low-spin potential energy surface. For PtF⁺ and PtCl⁺ with ethane, the main product is HF + HPt(C₂H₄)⁺ and HCl + HPt(C₂H₄)⁺, respectively. While for the PtBr⁺/C₂H₆ system, the final product is a mixture of HBr + HPt(C₂H₄)⁺ and H₂+BrPt(C₂H₄)⁺.

Keywords: Mechanism, DFT, Gas phase, C-H bond of C₂H₆ activation, Crossing point.

INTRODUCTION

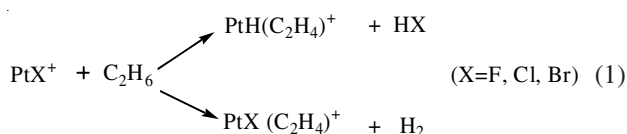
Alkane, as one of the most significant chemicals, has been extensively studied over the past decades due to its importance in immense scientific and organic synthesis¹. Hence, a great number of experiments combined with computational studies provide an efficient means to obtain a better insight into the reactivity patterns, the role of different ligands and the importance of aspects of electronic structure²⁻⁸. In particular, the activation of C-H and C-C bond of small alkane by bare transition metals as well as their ions in the gas phase has been the hot field of research that provides fundamental information on catalytic reaction mechanism, kinetics and thermodynamics⁹⁻¹⁴.

In 2008, Schroder and Schwarz observed the conceptual aspect that compare to the oversimplified bare metal atoms and their ions, there is a significant distinction in reactivity catalysis with respect to same metal assembling additional ligand¹⁵. Obviously, coordination of a metal by a covalently bound ligand X affects considerably the electronic structure and can be effectively control activation efficiency as well as nature of the chemical conversions to some extent¹⁶. The effect of halide ligands on the reactivity of 3d transition metal cations has been systematically studied. For instance, the observation that ground-state metal ions Cr⁺ does not reveal any reactivity toward saturated hydrocarbons¹⁷, whereas the CrCl⁺ could react with methane larger than propane. On the contrary, bare Fe⁺

activates small alkanes, but FeCl⁺ is completely inert in this respect¹⁸. By comparison, in the activation of C-H bond in alkane, the carbonyl complexes Fe(CO)⁺ and Cr(CO)⁺ are even less reactive than the bare metals¹⁹. In 2011, Maria Schlangen *et al.* have observed a good example to underline the ligand and substrate effects in gas-phase reactions of NiX⁺/RH couples (X = F, Cl, Br, ; R = CH₃, C₂H₅, C₃H₇, C₄H₉) in experimental²⁰ and theoretical²¹ aspects. The results show that, the halide metal cations NiX⁺ activation of C-H bond in ethane can be classified into two different categories: (a) bond activation of the organic substrate without obvious occurrence of Ni-X bond cleavage, that is, the losses of H₂, which formally leads to the corresponding NiX⁺/olefin complexes. (b) reactions involving Ni-X bond cleavage, namely the expulsions of HX, affording nickel-alkyl or nickel-alkenyl cations, respectively.

Recently, many scientists have reported the comprehensive study²²⁻²⁴ on reaction of ethane by metal ions Pt⁺. They found that Pt⁺ has strong catalytic effect on the activation reaction of ethane. To our best of knowledge, there is no theoretical and experimental study about ligand effects of X on Pt⁺. Therefore, in order to provide some useful information to experimentalists who are interested in this field, we have systematically carried out a theoretical investigation of the activation of C-H bond in ethane by PtX⁺ at the DFT level in this paper. Moreover, it is meaningful to explore how PtX⁺ differ from NiX⁺ in catalytic reactivity and reaction mechanism. To gain insight into the mechanism of the reaction of platinum PtX⁺ with ethane, we

present here computational studies on the reaction (1) and the detail of two possible mechanism (1,1- and 1,2-elimination) are considered.



COMPUTATIONAL METHODS

All calculations for the stationary points involved in ethane activation by gas-phase PtX^+ have been performed using the density functional theory (DFT) method based on the hybrid of Beckes three-parameter exchange functional and the Lee, Yang and Parr correlation functional (B3LYP)²⁵⁻²⁷. The large 6-311+G** basis set was performed using for C, H and X²⁸, the Stuttgart/Dresden (SDD) relativistic effective core potentials (ECP) were adopted to describe the role of Pt metal. Analytical frequency calculations at the same level of theory were performed in order to confirm the optimized structures to either a minimum or a first-order saddle point as well as to obtain the zero-point energy correction. Furthermore, intrinsic reaction coordinate (IRC) calculations²⁹ were performed to confirm that the optimized transition states correctly connect the relevant reactants and products. Natural population analysis was performed with natural bond orbital (NBO) analysis to gain further insight into the bonding properties³⁰. Single-point energy calculations were performed using the more rigorous CCSD and highly correlated MP2 approach at the B3LYP geometries. All computations reported here were carried out using the Gaussian 03³¹ and 09³² program suites.

RESULTS AND DISCUSSION

Reaction mechanism for PtX^+ (X = F, Cl and Br) with C_2H_6 : We discuss the mechanism of PtX^+ (X = F, Cl, Br,) in the activation process of C_2H_6 . Both high-spin and low-spin potential energy surfaces are characterized in detail. The energetics of intermediates and transition states, relative to the ground state reactants have been collected on the potential energy graphic. For the sake of simplicity, each species is labeled with its spin multiplicity as a superscript preceding the formula. For the convenience of our discussion in this article, some abbreviations ^aTS_b (a = 1,3, b = 1~10) represent transition states.

Reaction mechanism of PtF^+ with C_2H_6 : In the reaction mechanism of PtF^+ with ethane, both singlet and triplet states have been considered. The structures of the various critical points are depicted schematically in Fig. 1 and the calculated corresponding potential-energy surfaces (PESs) are shown in Fig. 2.

As shown in Fig. 1, in the triplet state, the reaction starts with the PtF^+ attaching to ethane to form a stable adduct complex ³FPt(C_2H_6)⁺, in which the C-H₍₁₎ bond is elongated from the calculated 1.093 Å for free ethane to 1.152 Å (hereafter, the primary, secondary and other activated hydrides are denoted as H₍₁₎, H₍₂₎, *etc.*), indicating existence of an agostic interaction between PtF^+ and ethane. The natural bond orbital

population of the valence electrons is $6s^{0.63}5d^{8.27}6p^{0.06}$ for the Pt center in ³FPt(C_2H_6)⁺. The low-spin ¹PtF⁺ with ethane tends to form an ¹FPtH(C_2H_5)⁺ intermediate directly, which has a natural bond orbital population of the valence electrons of $6s^{0.53}5d^{8.53}6p^{0.08}$ for the Pt center. (No encounter complex was found similar to the $\text{PtF}^+/\text{C}_2\text{H}_6$ system in the high-spin state). To confirm the calculated results, we used MP2/sdd/6-311+G** to calculate, but find the same one. Since the ¹Σ and ³Σ states of PtF^+ are practically isoenergetic, one can expect that, the minimal energy reaction pathway (MERP) may start at the molecular complex ¹FPtH(C_2H_5)⁺ from the corresponding ground reactants ¹PtF⁺ + C_2H_6 . From intermediate ¹FPtH(C_2H_5)⁺, the reaction is bifurcated as two pathways, which will take place according to both 1,2 and 1,1-elimination mechanism.

1,2-Elimination mechanism yielding HF and H₂: In the singlet states (Fig. 1), after the oxidative addition of the first C-H bond to PtF^+ , the next step is the migration of α-H from platinum to fluorine, meanwhile the β-H close to platinum *via* a four-member ¹TS2, leading to the intermediate ¹FHPt(C_2H_5)⁺ with a barrier of 0.84 kcal/mol, in which the Pt-F distance is elongated from 1.890 Å for ¹FPtH(C_2H_5)⁺ to 1.990 Å, β-C-H₍₂₎ bond is elongated from the calculated 1.093 Å for free ethane to 1.382 Å. The third step is the second hydrogen shift from β-carbon to platinum *via* ¹TS3 resulting in the complex ¹FHPtH(C_2H_4)⁺ with a barrier of 0.53 kcal/mol, which is the global-minimum structure on the singlet potential energy surface exothermic by 118.62 kcal/mol corresponding to the ground reactants. Moreover, these tiny energy differences between the transition states and the corresponding intermediates indicate that no true minimum was found for the C-H bond activation on the singlet surface. For ¹FHPtH(C_2H_4)⁺, the Pt-C bond distance is 2.12 Å, Pt-H distance is 1.51 Å, D_{H-Pt-C} = 90.25°. The natural bond orbital analysis reveals that the *d_s* orbitals of Pt have large contribution to the Pt-H bonds in ¹FHPtH(C_2H_4)⁺. As shown in Fig. 3, the Pt-C bond is formed from *p*(C) and *d_π*(Pt) in ¹FHPtH(C_2H_4)⁺. This interaction results in increasing the stability of the complex ¹FHPtH(C_2H_4)⁺. From the ¹FHPtH(C_2H_4)⁺, the reaction may divided into two pathways. The first pathway involve Pt-F bond cleavage, finally the ¹FHPtH(C_2H_4)⁺ adduct dissociates into the product ¹PtH(C_2H_4)⁺ + HF. The overall reaction is exothermic by 87.74 kcal/mol.

The other pathway include the dehydrogenation step, that may proceed as ¹FHPtH(C_2H_4)⁺ → ¹TS4 → ¹FPtH₂(C_2H_4)⁺ → ¹TS5 → ¹FPt(C_2H_4)(H₂)⁺ → ¹FPt(C_2H_4)⁺ + H₂. By comparison, there is a high barrier (46.34 kcal/mol) corresponding from the ¹FHPtH(C_2H_4)⁺ to the complex ¹FPtH₂(C_2H_4)⁺, which implies the reaction channel involving the elimination of H₂ is difficult to occur. Besides, the HF elimination channel is calculated to be exothermic (87.74 kcal/mol), which is larger than H₂ elimination channel (43.81 kcal/mol) on the overall reaction path. Thus, we can safely draw the conclusion that Pt-F bond cleavage channel is kinetically and thermodynamically feasible.

In the triplet state, from ³FPt(C_2H_6)⁺, the next step is the first C-H activation, a first hydrogen transfers from carbon to the metal Pt through ³TS1 leading to intermediate ³FPtH(C_2H_5)⁺ with an activation barrier of 10.47 kcal/mol. Subsequently, the Pt-H bond is cleaved and hydrogen atom transfers to F

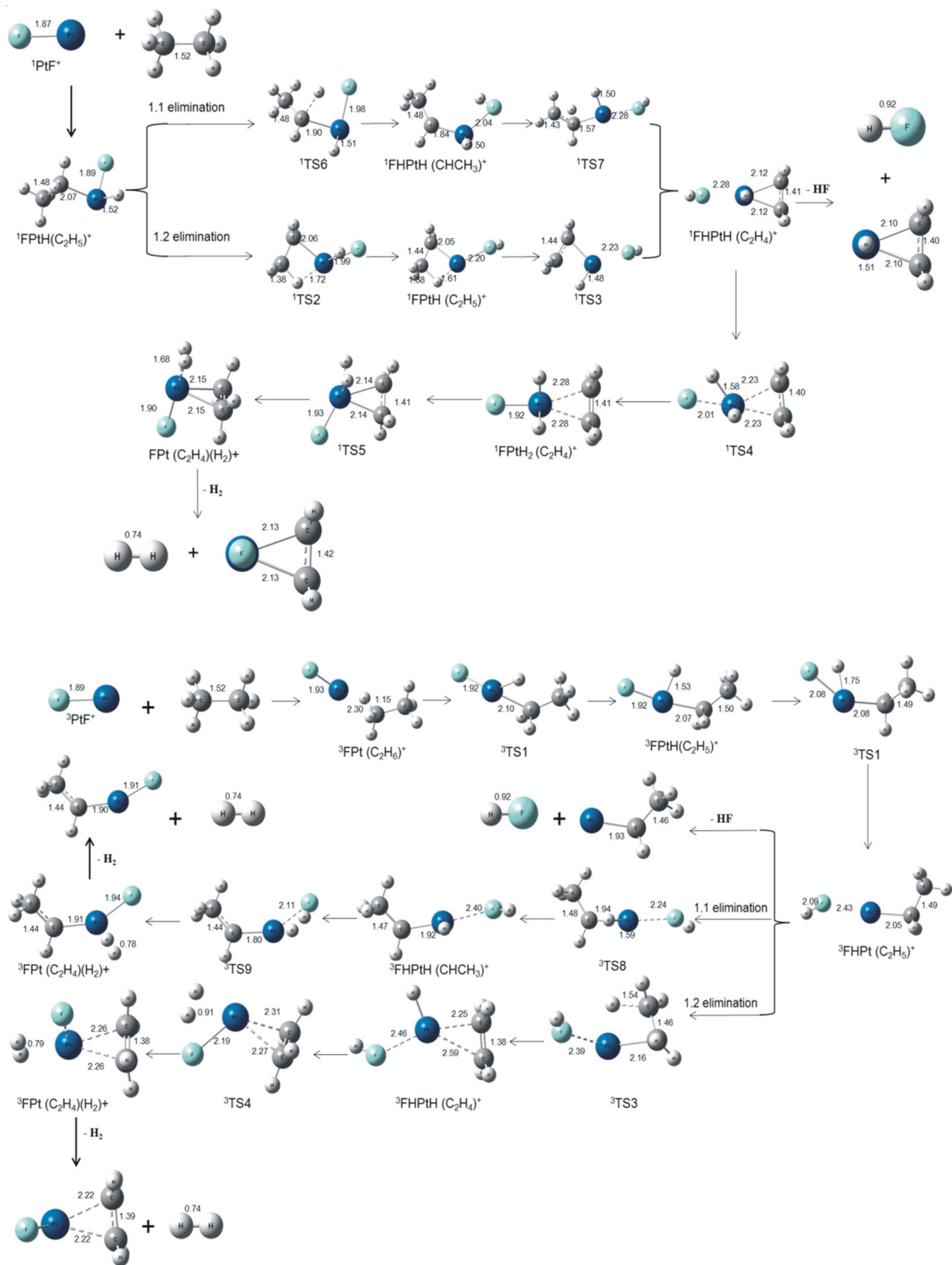


Fig. 1. Optimized geometries for the stationary points of the reaction $\text{PtF}^+ + \text{C}_2\text{H}_6 \rightarrow \text{FPt}(\text{C}_2\text{H}_4)^+ + \text{H}_2$, both in the singlet and triplet states (bond lengths in Å)

TABLE-I
VALENCE NATURAL BOND ORBITAL POPULATION OF Pt⁺ IN THESE COMPLEXES
ON 1-2 ELIMINATION POTENTIAL ENERGY SURFACES

1-2 Elimination States	PtF ⁺		PtCl ⁺		PtBr ⁺	
	¹ Σ	³ Σ	¹ Σ	³ Σ	¹ Σ	³ Σ
PtX ⁺	6s ^{0.04} 5d ^{8.57} 6p ^{0.03}	6s ^{0.34} 5d ^{8.29} 6p ^{0.02}	6s ^{0.09} 5d ^{8.80} 6p ^{0.05}	6s ^{0.46} 5d ^{8.60} 6p ^{0.03}	6s ^{0.16} 5d ^{8.77} 6p ^{0.04}	6s ^{0.49} 5d ^{8.71} 6p ^{0.04}
XPt(C ₂ H ₆) ⁺	6s ^{0.63} 5d ^{8.27} 6p ^{0.06}	6s ^{0.63} 5d ^{8.27} 6p ^{0.06}	6s ^{0.66} 5d ^{8.57} 6p ^{0.12}	6s ^{0.66} 5d ^{8.57} 6p ^{0.12}	6s ^{0.68} 5d ^{8.67} 6p ^{0.14}	6s ^{0.68} 5d ^{8.67} 6p ^{0.14}
TS1	6s ^{0.52} 5d ^{8.39} 6p ^{0.11}	6s ^{0.52} 5d ^{8.39} 6p ^{0.11}	6s ^{0.64} 5d ^{8.65} 6p ^{0.16}	6s ^{0.64} 5d ^{8.65} 6p ^{0.16}	6s ^{0.66} 5d ^{8.74} 6p ^{0.19}	6s ^{0.66} 5d ^{8.74} 6p ^{0.19}
XPtH(C ₂ H) ⁺	6s ^{0.53} 5d ^{8.53} 6p ^{0.08}	6s ^{0.62} 5d ^{8.42} 6p ^{0.10}	6s ^{0.61} 5d ^{8.75} 6p ^{0.14}	6s ^{0.66} 5d ^{8.67} 6p ^{0.18}	6s ^{0.61} 5d ^{8.81} 6p ^{0.15}	6s ^{0.67} 5d ^{8.76} 6p ^{0.18}
TS2	6s ^{0.56} 5d ^{8.79} 6p ^{0.10}	6s ^{0.69} 5d ^{8.42} 6p ^{0.06}	6s ^{0.55} 5d ^{8.95} 6p ^{0.17}	6s ^{0.61} 5d ^{8.65} 6p ^{0.11}	6s ^{0.54} 5d ^{9.03} 6p ^{0.17}	6s ^{0.60} 5d ^{8.70} 6p ^{0.13}
XHPt(C ₂ H ₅) ⁺	6s ^{0.46} 5d ^{9.05} 6p ^{0.02}	6s ^{0.60} 5d ^{8.52} 6p ^{0.02}	6s ^{0.54} 5d ^{9.09} 6p ^{0.09}	6s ^{0.64} 5d ^{8.58} 6p ^{0.05}	6s ^{0.56} 5d ^{9.11} 6p ^{0.11}	6s ^{0.78} 5d ^{8.53} 6p ^{0.07}
TS3	6s ^{0.48} 5d ^{9.03} 6p ^{0.02}	6s ^{0.40} 5d ^{8.66} 6p ^{0.20}	6s ^{0.60} 5d ^{9.07} 6p ^{0.11}	6s ^{0.49} 5d ^{8.72} 6p ^{0.29}	6s ^{0.63} 5d ^{9.08} 6p ^{0.12}	6s ^{0.52} 5d ^{8.75} 6p ^{0.32}
XHPtH(C ₂ H ₄) ⁺	6s ^{0.57} 5d ^{8.94} 6p ^{0.06}	6s ^{0.75} 5d ^{8.48} 6p ^{0.10}	6s ^{0.63} 5d ^{9.00} 6p ^{0.11}	6s ^{0.64} 5d ^{8.70} 6p ^{0.19}	6s ^{0.63} 5d ^{9.08} 6p ^{0.12}	6s ^{0.65} 5d ^{8.73} 6p ^{0.22}
TS4	6s ^{0.63} 5d ^{8.77} 6p ^{0.14}	6s ^{0.61} 5d ^{8.37} 6p ^{0.13}	6s ^{0.64} 5d ^{8.90} 6p ^{0.24}	6s ^{0.52} 5d ^{8.71} 6p ^{0.22}	6s ^{0.65} 5d ^{9.02} 6p ^{0.13}	6s ^{0.64} 5d ^{8.77} 6p ^{0.32}
XPtH ₂ (C ₂ H ₄) ⁺	6s ^{0.61} 5d ^{8.64} 6p ^{0.20}	6s ^{0.61} 5d ^{8.64} 6p ^{0.20}	6s ^{0.66} 5d ^{8.80} 6p ^{0.34}	6s ^{0.66} 5d ^{8.80} 6p ^{0.34}	6s ^{0.65} 5d ^{9.02} 6p ^{0.13}	6s ^{0.65} 5d ^{9.02} 6p ^{0.13}
TS5	6s ^{0.58} 5d ^{8.61} 6p ^{0.27}	6s ^{0.58} 5d ^{8.61} 6p ^{0.27}	6s ^{0.62} 5d ^{8.75} 6p ^{0.24}	6s ^{0.62} 5d ^{8.75} 6p ^{0.24}	6s ^{0.64} 5d ^{8.93} 6p ^{0.27}	6s ^{0.64} 5d ^{8.93} 6p ^{0.27}
XPt(C ₂ H ₄)(H ₂) ⁺	6s ^{0.44} 5d ^{8.68} 6p ^{0.18}	6s ^{0.63} 5d ^{8.27} 6p ^{0.06}	6s ^{0.49} 5d ^{8.83} 6p ^{0.29}	6s ^{0.54} 5d ^{8.64} 6p ^{0.29}	6s ^{0.51} 5d ^{8.86} 6p ^{0.33}	6s ^{0.56} 5d ^{8.72} 6p ^{0.34}
XPt(C ₂ H ₄)(H ₂)	6s ^{0.54} 5d ^{8.89} 6p ^{0.02}	6s ^{0.58} 5d ^{8.30} 6p ^{0.08}	6s ^{0.42} 5d ^{8.86} 6p ^{0.33}	6s ^{0.51} 5d ^{8.69} 6p ^{0.27}	6s ^{0.48} 5d ^{8.92} 6p ^{0.30}	6s ^{0.52} 5d ^{8.78} 6p ^{0.32}

similar, clearly showing that the similarity in bonding property.

For the PtCl⁺/C₂H₆ system, in the singlet state, the molecular complex ¹CIPtH(C₂H₅)⁺ lies 52.14 kcal/mol below the ground-state reactants. The natural bond orbital population of the valence electrons is 6s^{0.61}5d^{8.75}6p^{0.14} for the Pt center in ¹CIPtH(C₂H₅)⁺, with the Pt–C distance of 2.053 Å. The high-spin ³CIPt(C₂H₆)⁺ complex lies 15.17 kcal/mol higher in energy than the low-spin ¹CIPtH(C₂H₅)⁺, which has a natural bond orbital population of the valence electrons of 6s^{0.66}5d^{8.57}6p^{0.12} for the Pt center. ³CIPt(C₂H₆)⁺ has the Pt–C distance of 2.275 Å,

which is larger than that of ¹CIPtH(C₂H₅)⁺. As depicted in Fig. 4, a curve crossing from the triplet state to the singlet state is required somewhere before formation the encounter complex. In order to search the crossing point, an approach suggested by Zhang *et al.*³³ and Yoshizawa *et al.*³⁴ for approximately locating the crossing point of two potential-energy surfaces of different multiplicities has been used. As shown in Fig. 5(a), the crossing point has the Pt–C distance of 3.25 Å.

Let us look at the 1,2-elimination mechanism in the singlet state, after formation of the encounter complex ¹CIPtH(C₂H₅)⁺. The second reaction step is associated with the migration of

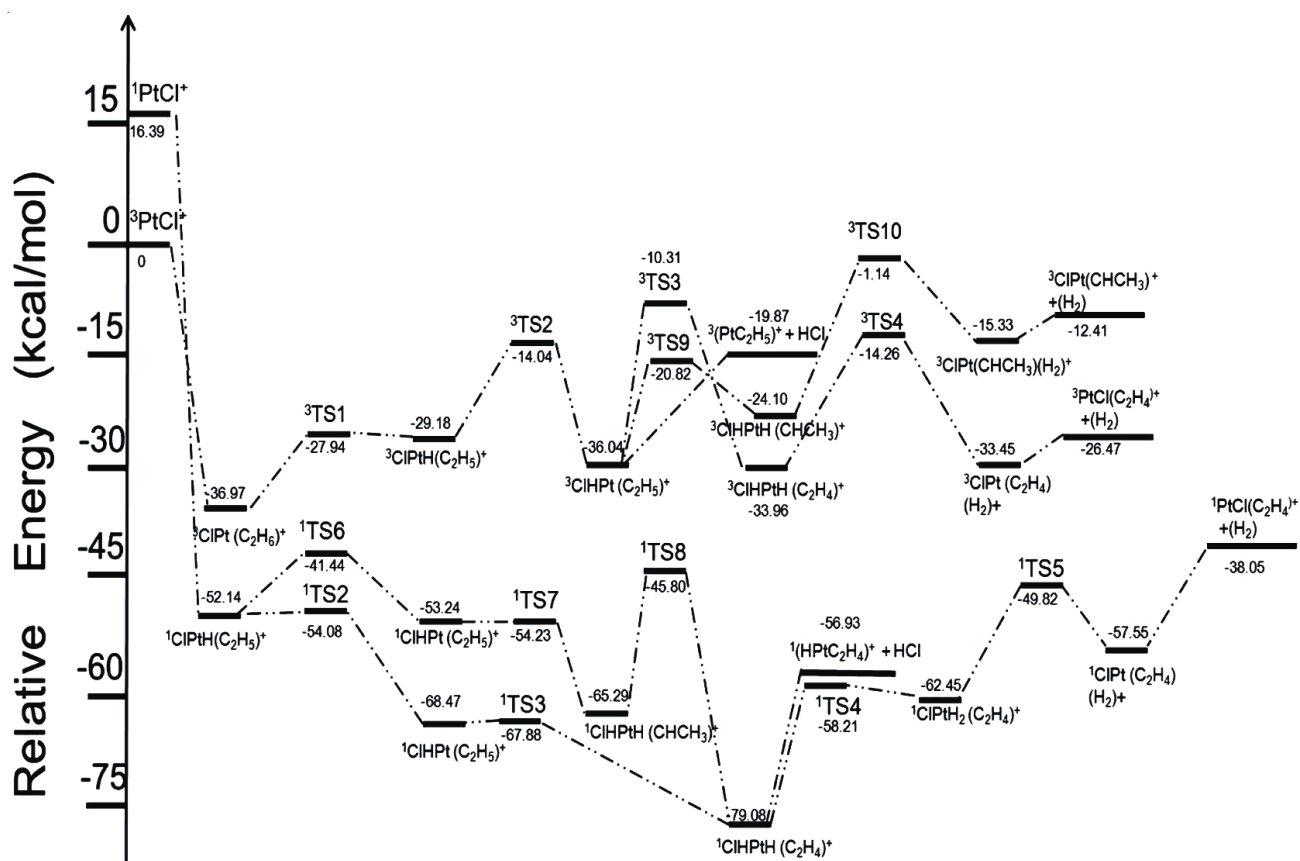


Fig. 4. Potential energy surfaces of the reactions PtCl⁺ + C₂H₆ in both low and high-spin states

an H atom from Pt to Cl through $^1\text{TS2}$ to form the complex $^1\text{ClHPt}(\text{C}_2\text{H}_5)^+$. Then the reaction is associated with the Pt-H₍₂₎ bond formation cooperated with the C-H₍₂₎ bond breaking *via* $^1\text{TS3}$, yielding the global-minimum structure $^1\text{ClHPtH}(\text{C}_2\text{H}_4)^+$ that serves as the direct precursor for loss of the HCl. The natural bond orbital calculations show that the $^1\text{ClHPtH}(\text{C}_2\text{H}_4)^+$ has a valence electrons population of $6s^{0.63}5d^{9.00}6p^{0.11}$ for the Pt center, of which the Pt-C bond is consist of platinum $5d$ (mainly is d_{xz}) orbital and carbon p orbital. The energies of $^1\text{TS2}$ and $^1\text{TS3}$ are all very close to those of the early complex $^1\text{ClPtH}(\text{C}_2\text{H}_5)^+$ and $^1\text{ClHPt}(\text{C}_2\text{H}_5)^+$ respectively. These results indicate that the transition states might be negligible on the overall low-spin reaction path. The results listed in Fig. 4 indicate that $^1\text{ClHPtH}(\text{C}_2\text{H}_4)^+$ (which is 79.08 kcal/mol below the entrance channel) is 45.11 kcal/mol lower in energy than $^3\text{ClHPtH}(\text{C}_2\text{H}_4)^+$. It is due to the large difference in binding of $\text{ClHPtH}(\text{C}_2\text{H}_4)^+$. In the low spin state, the Pt⁺ is capable of forming covalent bond with hydrogen and the ethylene group, yielding the three membered ring structure (there are nine electrons in these bonding orbitals), whereas a triplet state need these electrons shift to a nonbonding orbital. Thus, the bonding is stronger in the singlet state. From the $^1\text{ClHPtH}(\text{C}_2\text{H}_4)^+$, two processes are located to produce the two products. One is followed the Pt-Cl bond cleavage to yield the stable product $^1\text{HPt}(\text{C}_2\text{H}_4)^+ + \text{HCl}$. The other channels followed by the reductive elimination step to release a H₂ molecule. Due to the exit channel to form $^1\text{HPt}(\text{C}_2\text{H}_4)^+$ and HCl are more exothermic (18.88 kcal/mol) than the dehydrogenation one, indicating that the formation of HCl is easier than H₂.

Now, we will turn to the 1,1-elimination mechanism in singlet state. After the first C-H insertion product $^1\text{ClPtH}(\text{C}_2\text{H}_5)^+$ is formed, followed by successive H-transfer step from the Pt to Cl *via* $^1\text{TS6}$ to form $^1\text{ClHPt}(\text{C}_2\text{H}_5)^+$, (this step is not like the case of $\text{PtF}^+/\text{C}_2\text{H}_6$, but very similar to the $\text{PtBr}^+/\text{C}_2\text{H}_6$ system) with a barrier of 10.69 kcal/mol. The second C-H₍₂₎ bond activation process through $^1\text{TS7}$ for the H₍₂₎ transfer to platinum, which formation of intermediate $^1\text{ClHPtH}(\text{CHCH}_3)^+$ with an almost negligible activation barrier (0.99 kcal/mol). Later, the migration of a third hydrogen occurs to give the common complex $^1\text{ClHPtH}(\text{C}_2\text{H}_4)^+$ *via* $^1\text{TS8}$ with barrier of 19.48 kcal/mol. Since the activation energies of 1,1-elimination are all higher than that of 1,2-elimination in both states. Hence, we predict that if the reaction is carried out at room temperature, the most competitive channel should be 1,2-elimination one. Like PtCl^+ , the ground state of PtBr^+ is also the triplet state, which lies 23.90 kcal/mol lower in energy than the singlet state. The triplet complex $^3\text{BrPt}(\text{C}_2\text{H}_6)^+$ lies 13.83 kcal/mol higher than the singlet one. These results show that PtBr^+ , C_2H_6 activation starting from the ground-state reactants also needs the spin inversion processes (similar to the case of $\text{PtCl}^+ + \text{C}_2\text{H}_6$). As shown in Fig. 5(b), the minimum on the seam of crossings is close to the reactants (the Pt-C distance is 2.90 Å), which is shorter than the crossing point of $\text{PtCl}^+/\text{C}_2\text{H}_6$ system.

Since the mechanism of the reaction are very similar to the $\text{PtCl}^+/\text{C}_2\text{H}_6$ system, we do not discuss their geometries in further detail but show some differences. It can be seen from the minimum energy path in the reaction (1,2-elimination in the singlet state), compared to the case of $\text{PtCl}^+ + \text{C}_2\text{H}_6$, there

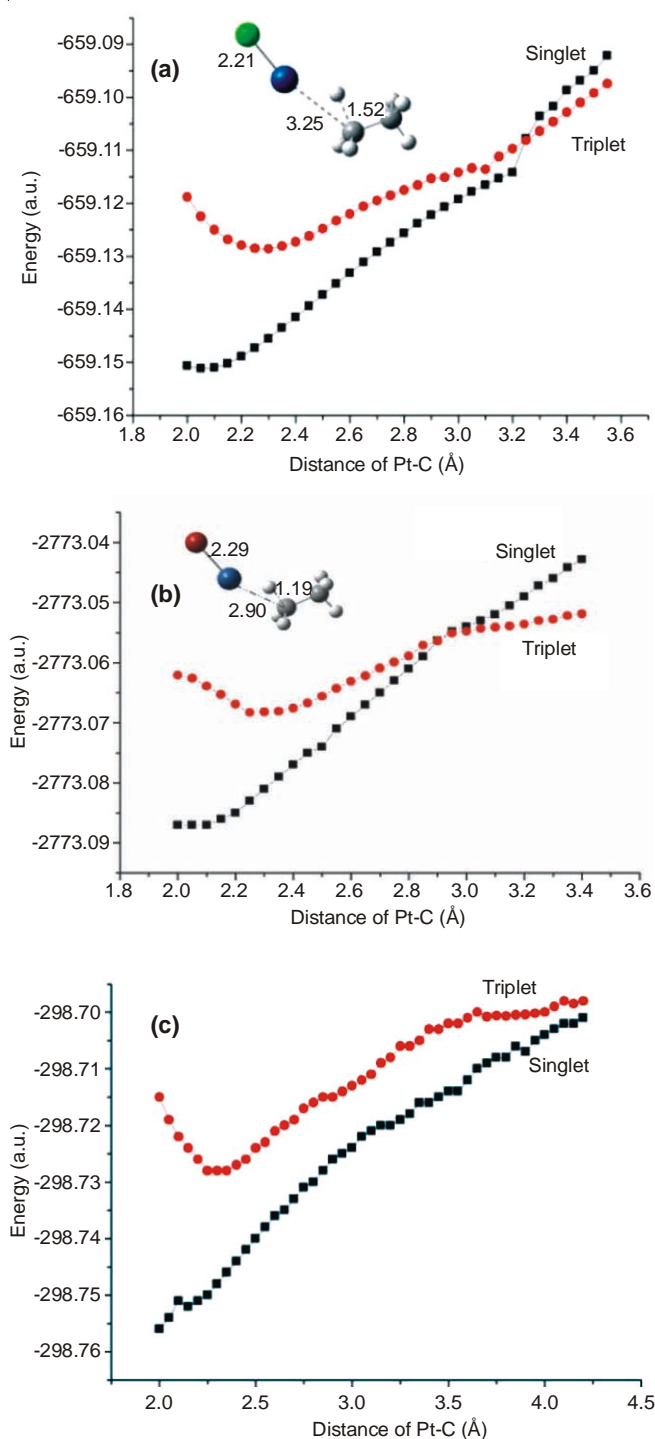


Fig. 5. Singlet and triplet potential energies of the reactant complex as a function of the distance between PtCl^+ (a)/ PtBr^+ (b)/ PtF^+ (c) and carbon atom of C_2H_6

there exist the smaller energy (8.51 kcal/mol) difference between the products of $\text{HPt}(\text{C}_2\text{H}_4)^+ + \text{HBr}$ and $\text{H}_2 + \text{BrPt}(\text{C}_2\text{H}_4)^+$. In addition, these two exit channels are situated at more than 30 kcal/mol below the entrance channel, so it can be performed spontaneously at room temperature. Therefore it is likely that among the major channel (1,2-elimination) for the reaction of PtBr^+ with C_2H_6 , the two reaction paths will occur in parallel to give the final product is a mixture of $\text{HBr} + \text{HPt}(\text{C}_2\text{H}_4)^+$ and $\text{H}_2 + \text{BrPt}(\text{C}_2\text{H}_4)^+$.

From the minimum energy pathways of the reaction of PtX⁺ (X = F, Cl, Br) and ethane, since the energies of the intermediates and transition states all are lower than the ground reactant, the PtF⁺, PtCl⁺ and PtBr⁺ are likely to be excellent mediators for C₂H₆ activation. Originally, the first H atom migrate to the halogen atom, forming the intermediate XHPt(C₂H₅)⁺. Then, the second C-H bond activation will occur to form the global-minimum structure in concert with the migration of a second hydrogen from C₂H₅ to the metal yields XHPtH(C₂H₄)⁺. The Pt-X bond cleavage products of the reaction of PtX⁺ and ethane are all the three membered ring complex PtH(C₂H₄)⁺. The exothermicities of the reactions are 87.74, 56.93 and 39.36 kcal/mol for PtF⁺, PtCl⁺ and PtBr⁺, respectively.

Crossing points between potential-energy surfaces of different multiplicities: To gain a better understanding of the spin inversion processes described above, it is meaningful to discuss the crossing points between the singlet and triplet states potential-energy surfaces, on the reaction pathways. It can be seen from Fig. 4, the ground state of PtCl⁺ is triplet state, which lies 16.39 kcal/mol lower in energy than the singlet reactant, but the triplet encounter complex ¹ClPt(C₂H₆)⁺ lies 15.17 kcal/mol higher in energy than the singlet one. These results show that the intersystem crossing arises before the formation of first complex. If spin inversion to the singlet potential-energy surface is involved, the energy barrier is greatly decreased in the later parts of the reaction path. As a function of the distance between Pt of PtCl⁺ and C of C₂H₆ is depicted in Fig. 5(a). For a given Pt-C bond length, all geometrical degrees of freedom are optimized for each electronic state, the triplet and singlet curves cross at the point Pt-C bond length of 3.25 Å. For the case of PtBr⁺/C₂H₆, which have the same properties, as C₂H₆ approaches PtBr⁺, the triplet and singlet curves cross at the point Pt-C bond length of 2.90 Å, it can be seen from Fig. 5(b).

However, for the PtF⁺/C₂H₆ system, the ground state of PtF⁺ is the singlet state, which lies only 1.02 kcal/mol higher in energy than the triplet state. This result indicate that the reaction will starting from the singlet PtF⁺, C₂H₆ activation proceeds rather quickly cross over to the low spin potential-energy surface. As a consequence, no crossing point between

the triplet and singlet potential-energy surfaces occurs in the PtF⁺/C₂H₆ system. In order to validate this point, we also scan the Pt-C bond in PtF⁺/C₂H₆ system, as depicted in Fig. 5(c) that the complex in the high spin state are always higher in energy than that the low spin state, until the Pt-C bond get long enough to the reactant (in which the both state molecular complexes FPt(C₂H₆)⁺ are practically isoenergetic). These calculated results show that the reaction of PtF⁺ + C₂H₆ proceeding on the singlet potential-energy surface with a spin-allowed manner.

As discussed above, since the different effects of the X ligands on PtX⁺, the Pt-C distances of the XPt(C₂H₆)⁺ (X = F, Cl, Br) complex at the crossing point become longer from Br to F. As PtBr⁺/C₂H₆ system, the Pt-C distance is 2.90 Å (close to the Pt-C bond of the stationary point ³BrPt(C₂H₆)⁺ in the triplet state); for PtCl⁺/C₂H₆ system, the Pt-C distance is 3.25 Å [longer than the Pt-C bond of ClPt(C₂H₆)⁺ in the triplet state]; even if the Pt-C distance is longer than 4 Å, the PtF(C₂H₆)⁺ complex of both state(triplet and singlet) are still isoenergetic. Under this property of the crossing point, if we assumed that the ground state of PtF⁺ is the triplet state, the Pt-C distance is much longer than that in the triplet state encounter complex FPt(C₂H₆)⁺, which reactivity routes are quite similar to the course of PtH/CH₄³⁵. That is to say, the crossing point becomes step by step closer to the reactant from Br to F.

Single-point energies: In order to verify the accuracy of the results, we also performed using the more rigorous CCSD³⁶ method and highly correlated MP2 approach to calculate the single-point energy of the species in 1,2-elimination potential energy surfaces at the B3LYP geometries. The energies relative to high-spin PtX⁺/C₂H₆ are shown in Table-2. The MP2 and CCSD results reveal that the energy of activation for the second C-H bond in the case of PtCl⁺/C₂H₆ is negligible, 0.57 kcal/mol for CCSD and 0.63 kcal/mol for MP2; these energies are in good agreement with B3LYP result of 0.59 kcal/mol. In like manner, the calculated energy of ¹TS2 in the PtBr⁺/C₂H₆ system, 3.83 kcal/mol relative to ¹BrPt(C₂H₆)⁺ from CCSD, compares well with the 2.31 kcal/mol energy of ¹TS2 relative to ¹BrPt(C₂H₆)⁺ for B3LYP. The good agreement between the B3LYP energies and the results obtained using the MP2 and

TABLE-2
SINGLE-POINT ENERGIES (kcal/mol) OF THE SPECIES ON THE 1-2 ELIMINATION POTENTIAL ENERGY SURFACES OF THE REACTIONS PtX⁺ (X = F, Cl AND Br) + C₂H₆ FROM DFT-OPTIMIZED STRUCTURES

1-2 Elimination	PtF ⁺				PtCl ⁺				PtBr ⁺					
	States		¹ Σ		³ Σ		¹ Σ		³ Σ		¹ Σ		³ Σ	
Species	MP2	CCSD	MP2	CCSD	MP2	CCSD	MP2	CCSD	MP2	CCSD	MP2	CCSD	MP2	CCSD
XPt(C ₂ H ₆) ⁺	-	-	0.00	0.00	-	-	0.00	0.00	-	-	0.00	0.00	-	-
TS1	-	-	33.63	29.49	-	-	15.43	16.94	-	-	8.38	18.82	-	-
XPtH(C ₂ H ₅) ⁺	-26.66	-18.19	12.36	11.92	-25.91	-30.77	13.99	15.68	-42.16	-34.92	8.75	15.06	-	-
TS2	-25.48	-16.86	42.92	33.25	-28.31	-33.06	28.36	32.00	-45.99	-31.29	16.69	23.25	-	-
XHPt(C ₂ H ₅) ⁺	-72.22	-61.87	-15.56	-16.31	-47.69	-48.94	17.75	20.70	-54.78	-44.47	-4.39	-11.92	-	-
TS3	-72.26	-61.83	-4.58	-3.13	-47.06	-48.37	22.46	27.61	-54.09	-42.59	14.81	25.39	-	-
XHPtH(C ₂ H ₄) ⁺	-85.59	-76.55	-21.52	-23.84	-57.47	-65.26	0.56	1.31	-63.81	-45.14	-6.14	-12.29	-	-
TS4	-36.33	-20.70	15.87	18.19	-37.88	-45.80	25.97	31.00	-53.15	-36.94	12.48	23.06	-	-
XPtH ₂ (C ₂ H ₄) ⁺	-49.57	-36.39	-	-	-43.54	-38.86	-	-	-56.91	-42.59	-	-	-	-
TS5	-43.54	-26.35	-	-	-33.57	-45.18	-	-	-45.93	-38.78	-	-	-	-
XPt(C ₂ H ₄)(H ₂) ⁺	-45.49	-35.76	0.81	2.51	-34.19	-28.86	5.45	9.41	-45.68	-34.23	-12.23	-10.35	-	-
XPt(C ₂ H ₄)(H ₂)	-3.62	5.83	9.23	11.23	-18.26	-12.33	13.86	14.03	-29.38	-20.31	-6.08	-4.23	-	-

CCSD method indicate that B3LYP is feasible for modeling the reaction of $\text{PtX}^+/\text{C}_2\text{H}_6$ systems. Additionally, we use the B3LYP as the basis of most of our discussion, because we have more experience with this method and more confidence in its comparison with experimental results for the identification of congener molecules³⁷.

Comparison among the reactions of NiX^+ ($\text{X} = \text{F}, \text{Cl}, \text{Br}$) + C_2H_6 : We also summarize the findings of both our work and previous studies concerning the behaviour of the potential-energy surfaces for the ethane activation by first-row halides diatomic cations NiX^+ ($\text{X} = \text{F}, \text{Cl}, \text{Br}$), the reaction paths and the geometric structures of key points have many features in common, especially along the low-spin-state potential-energy surfaces. Despite the qualitative similarities among the reaction paths, there are also have fundamental differences exist. For the ion molecule reaction of NiX^+ ($\text{X} = \text{F}, \text{Cl}$) with ethane, the experimental²⁰ and theoretical results²¹ detects the major products are $\text{Ni}(\text{C}_2\text{H}_5)^+$ and HX ($\text{X} = \text{F}, \text{Cl}$). As for these aspects, our values show that the third-row halide PtX^+ ($\text{X} = \text{F}, \text{Cl}$) and ethane agree well with the previous studies of first-row congeners reactions. However, for the $\text{NiBr}^+/\text{C}_2\text{H}_6$ systems, the channel for giving products of $\text{Ni}(\text{C}_2\text{H}_5)^+ + \text{HBr}$ is negligible due to the larger barrier and energy requirement compared to the dehydrogenation one. This indicates that the pathways leading to $\text{Ni}(\text{C}_2\text{H}_5)^+ + \text{HBr}$ products are uncompetitive. As a consequence, reflected in the final product distributions, $\text{NiBr}(\text{C}_2\text{H}_4)^+$ and H_2 are the main products. Whereas for the $\text{PtBr}^+/\text{C}_2\text{H}_6$ couple, our results show that there is small difference in energy between the two exit channels, which are situated at more than 30 kcal/mol below reactant energy. According to the gas phase experiment carried out at relatively low pressure and with very

high reaction coefficients, all these reactions take place at constant energy and angular momentum³⁸. The final product is a mixture of $\text{HBr} + \text{HPt}(\text{C}_2\text{H}_4)^+$ and $\text{H}_2 + \text{BrPt}(\text{C}_2\text{H}_4)^+$.

The second difference is actual mechanism of the reaction. In the process of the reactions of NiX^+ and ethane, with the formation of $\text{XHNiH}(\text{C}_2\text{H}_4)^+$, a subsequent back transfer of a hydrogen atom from HX to the hydride ligand through a concerted reaction to give the $\text{XNi}(\text{C}_2\text{H}_4)(\text{H}_2)^+$ complex. However, for the $\text{PtX}^+/\text{C}_2\text{H}_6$ couple, from the $\text{XHPtH}(\text{C}_2\text{H}_4)^+$, the hydrogen atom from halogen shifts to the metal, then the two H atoms on the Pt rearrange to form the $\text{XPt}(\text{C}_2\text{H}_4)(\text{H}_2)^+$ complex, in which Pt^+ is capable of forming the stable three membered ring structure (in which the electron state of Pt^+ is singlet), which reveal that the low-spin state of the PtX^+ ($\text{X} = \text{F}, \text{Cl}, \text{Br}$) is more stable.

Conclusion

Two possible mechanisms (1,1- and 1,2-elimination) of ethane activation by the halide platinum ions PtX^+ ($\text{X} = \text{F}, \text{Cl}, \text{Br}$) have been investigated theoretically at the DFT (B3LYP) level and based on the above mentioned basis set (RECP+6-311+G**). Both high-spin and low-spin potential energy surfaces have been characterized in detail. Some comparisons with our work and first-row congeners have been performed. The following conclusions can be drawn from the present work: First, the activation energy barriers of reactions are located energetically below the entrance and exit channels, thus PtX^+ could be regard as the good mediators for the activity of ethane. Second, since the energies of the intermediates and transition states in the singlet state are all lower than the triplet ones, the reaction takes place more easily along the low-spin potential

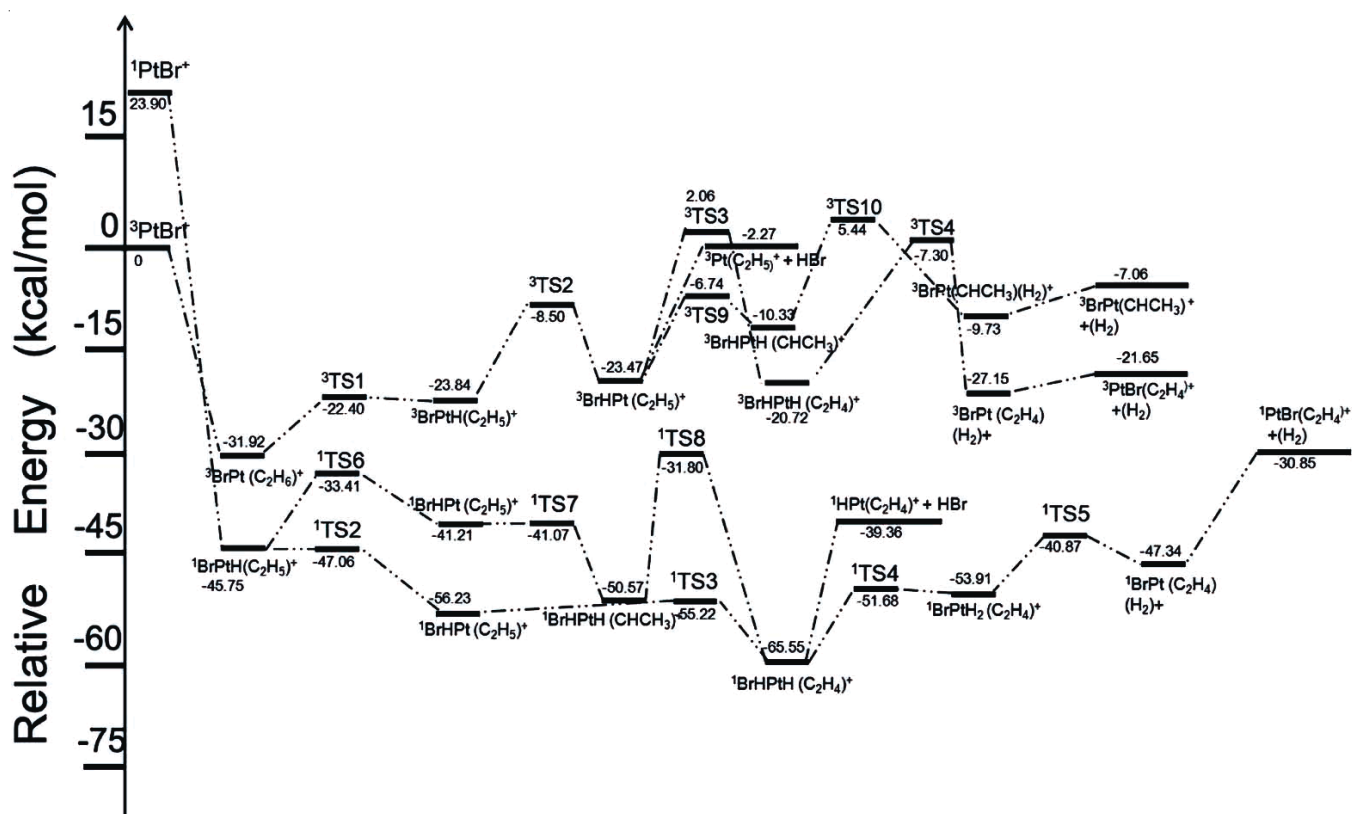


Fig. 6. Potential energy surfaces of the reactions $\text{PtBr}^+ + \text{C}_2\text{H}_6$ in both low and high-spin states

energy surface. Moreover, For PtCl⁺/C₂H₆ and PtBr⁺/C₂H₆ systems, an intersystem crossing from the triplet to singlet states is required and the minimum crossing point can be approximately viewed as the reactants. In comparison, the PtF⁺/C₂H₆ couple proceeds on the ground-state potential energy surface with a spin-allowed manner.

With the substantial differences in exothermicity and energy barriers in formation of products provide a rational basis to justify the conclusions that in the case of PtX⁺/C₂H₆ (X = F, Cl), the main product is HF + HPt(C₂H₄)⁺ and HCl + HPt(C₂H₄)⁺, respectively. For the PtBr⁺/C₂H₆ system, the final product is a mixture of HBr + HPt(C₂H₄)⁺ and H₂+BrPt(C₂H₄)⁺.

ACKNOWLEDGEMENTS

The authors acknowledge computing resources and time on the Supercomputing Center of Cold and Arid Region Environment and Engineering Research Institute of Chinese Academy of Sciences, Gansu Province Supercomputer Center and Institute of Functional Material Chemistry of Northeast Normal University for essential support.

REFERENCES

1. K. Othmer, Encyclopedia of Chemical Technology, Wiley, New York (1991).
2. M. Pecul and T. Helgaker, *Int. J. Mol. Sci.*, **4**, 143 (2003).
3. P. Ye, Q. Ye, G.B. Zhang and Z. Cao, *Chem. Phys. Lett.*, **501**, 554 (2011).
4. Y. Joshi and K.T. Thomson, *J. Catal.*, **246**, 249 (2007).
5. D.K. Bohme and H. Schwarz, *Angew. Chem. Int. Ed.*, **44**, 2336 (2005).
6. D. Schroder and H. Schwarz, Topics in Organometallic Chemistry, Springer-Verlag: Berlin, Heidelberg (2007).
7. K. Eller and H. Schwarz, *Chem. Rev.*, **91**, 1121 (1991).
8. J. Roithová and D. Schröder, *Chem. Rev.*, **110**, 1170 (2010).
9. S.H. Zhang, S. Li and Y. Jiang, *Organometallics*, **22**, 3820 (2003).
10. M.C. Holthausen and W. Koch, *J. Am. Chem. Soc.*, **118**, 9932 (1996).
11. G.T. De Jong, D.P. Geerke, A. Diefenbach, M. Solà and F.M. Bickelhaupt, *J. Comput. Chem.*, **26**, 1006 (2005).
12. D. Schroder and H. Schwarz, *Angew. Chem. Int. Ed.*, **34**, 1973 (1995).
13. A. Yakovlev, A. Shubin, G. Zhidomirov and R.A. Van Santen, *Catal. Lett.*, **70**, 175 (2000).
14. Á. Révész, P. Milko, J. Zabka, D. Schröder and J. Roithová, *J. Mass Spectrom.*, **45**, 1246 (2010).
15. D. Schroder and H. Schwarz, *Proc. Natl. Acad. Sci. USA*, **105**, 18114 (2008).
16. M. Schlangen, D. Schröder and H. Schwarz, *Chem. Eur. J.*, **13**, 6810 (2007).
17. L.F. Halle, P.B. Armentrout and J.L. Beauchamp, *Organometallics*, **1**, 963 (1982).
18. M.L. Mandich, M.L. Steigerwald and W.D. Reents, *J. Am. Chem. Soc.*, **108**, 6197 (1986).
19. P.B. Armentrout and B.L. Tjelta, *Organometallics*, **16**, 5372 (1997).
20. M. Schlangen and H. Schwarz, *J. Catal.*, **284**, 126 (2011).
21. M. Schlangen, Dissertation D83, Nickel-Mediated Bond Activation of Small Alkanes and of Molecular Oxygen-Ligand Effects and The Role of the Metal's Formal Oxidation State, Technische Universität Berlin, (2008).
22. R.M. Watwe, B.E. Spiewak and R.D. Cortright, *J. Catal.*, **180**, 184 (1998).
23. T. Hanmura, M. Ichihashi and T. Kondow, *J. Phys. Chem. A*, **106**, 11465 (2002).
24. C. Adlhart and E. Uggerud, *Chem. Eur. J.*, **13**, 6883 (2007).
25. A.D. Becke, *Phys. Rev.*, **38**, 3098 (1988).
26. A.D. Becke, *J. Chem. Phys.*, **98**, 5648 (1993).
27. C. Lee, W. Yang and R.G. Parr, *Phys. Rev.*, **37**, 785 (1988).
28. M.J. Frisch, J.A. Pople and J.S. Binkley, *J. Chem. Phys.*, **80**, 3265 (1984).
29. W. Lewis-Bevan, R.D. Gaston, J. Tyrrell, W.D. Stork and G.L. Salmon, *J. Am. Chem. Soc.*, **114**, 1933 (1992).
30. A.E. Reed, R.B. Weinstock and F. Weinhold, *J. Chem. Phys.*, **83**, 735 (1985).
31. M.J. Frisch, G.W. Trucks, H.B. Schlegel, G.E. Scuseria, M.A. Robb, J.R. Cheeseman, J.A. Montgomery Jr., T. Vreven, K.N. Kudin, J.C. Burant, J.M. Millam, S.S. Iyengar, J. Tomasi, V. Barone, B. Mennucci, M. Cossi, G. Scalmani, N. Rega, G.A. Petersson, H. Nakatsuji, M. Hada, M. Ehara, K. Toyota, R. Fukuda, J. Hasegawa, M. Ishida, T. Nakajima, Y. Honda, O. Kitao, H. Nakai, M. Klene, X. Li, J.E. Knox, H.P. Hratchian, J.B. Cross, V. Bakken, C. Adamo, J. Jaramillo, R. Gomperts, R.E. Stratmann, O. Yazyev, A.J. Austin, R. Cammi, C. Pomelli, J.W. Ochterski, P.Y. Ayala, K. Morokuma, G.A. Voth, P. Salvador, J.J. Dannenberg, V.G. Zakrzewski, S. Dapprich, A.D. Daniels, M.C. Strain, O. Farkas, D.K. Malick, A.D. Rabuck, K. Raghavachari, J.B. Foresman, J.V. Ortiz, Q. Cui, A.G. Baboul, S. Clifford, J. Cioslowski, B.B. Stefanov, G. Liu, A. Liashenko, P. Piskorz, I. Komaromi, R.L. Martin, D.J. Fox, T. Keith, M.A. Al-Laham, C.Y. Peng, A. Nanayakkara, M. Challacombe, P.M.W. Gill, B. Johnson, W. Chen, M.W. Wong, C. Gonzalez and J.A. Pople, Gaussian 03, revision c. 02; Gaussian, Inc., Wallingford, CT (2004).
32. M.J. Frisch, G.W. Trucks, H.B. Schlegel, G.E. Scuseria, M.A. Robb, J.R. Cheeseman, G. Scalmani, V. Barone, B. Mennucci, G.A. Petersson, H. Nakatsuji, M. Caricato, X. Li, H.P. Hratchian, A.F. Izmaylov, J. Bloino, G. Zheng, J.L. Sonnenberg, M. Hada, M. Ehara, K. Toyota, R. Fukuda, J. Hasegawa, M. Ishida, T. Nakajima, Y. Honda, O. Kitao, H. Nakai, T. Vreven, J.A. Montgomery, Jr., J.E. Peralta, F. Ogliaro, M. Bearpark, J.J. Heyd, E. Brothers, K.N. Kudin, V.N. Staroverov, R. Kobayashi, J. Normand, K. Raghavachari, A. Rendell, J. C. Burant, S.S. Iyengar, J. Tomasi, M. Cossi, N. Rega, J.M. Millam, M. Klene, J.E. Knox, J.B. Cross, V. Bakken, C. Adamo, J. Jaramillo, R. Gomperts, R.E. Stratmann, O. Yazyev, A.J. Austin, R. Cammi, C. Pomelli, J.W. Ochterski, R.L. Martin, K. Morokuma, V.G. Zakrzewski, G.A. Voth, P. Salvador, J.J. Dannenberg, S. Dapprich, A.D. Daniels, Ö. Farkas, J.B. Foresman, J.V. Ortiz, J. Cioslowski and D.J. Fox, Gaussian 09, Revision D.01, Gaussian, Inc., Wallingford, CT (2009).
33. G. Zhang, S. Li and Y. Jiang, *Organometallics*, **22**, 3820 (2003).
34. K. Yoshizawa, Y. Shiota and T. Yamabe, *J. Chem. Phys.*, **111**, 538 (1999).
35. S.L. Liu, Z.Y. Geng, Y. Wang and Y. Yan, *J. Phys. Chem. A*, **116**, 4560 (2012).
36. G.D. Purvis III and R.J. Bartlett, *J. Chem. Phys.*, **76**, 1910 (1982).
37. H.G. Cho and L. Andrews, *Organometallics*, **28**, 1358 (2009).
38. J. Zhou, Z.Y. Geng, J. Liu, Y. Wang, X. Wang, J. Wu and H. Liu, *Comput. Theoret. Chem.*, **965**, 221 (2011).